Chem

CellPress

Article

Unprecedented *endo*-oxidative cyclometallation and [4 + 3] cycloaddition of diene-vinylcyclopropanes

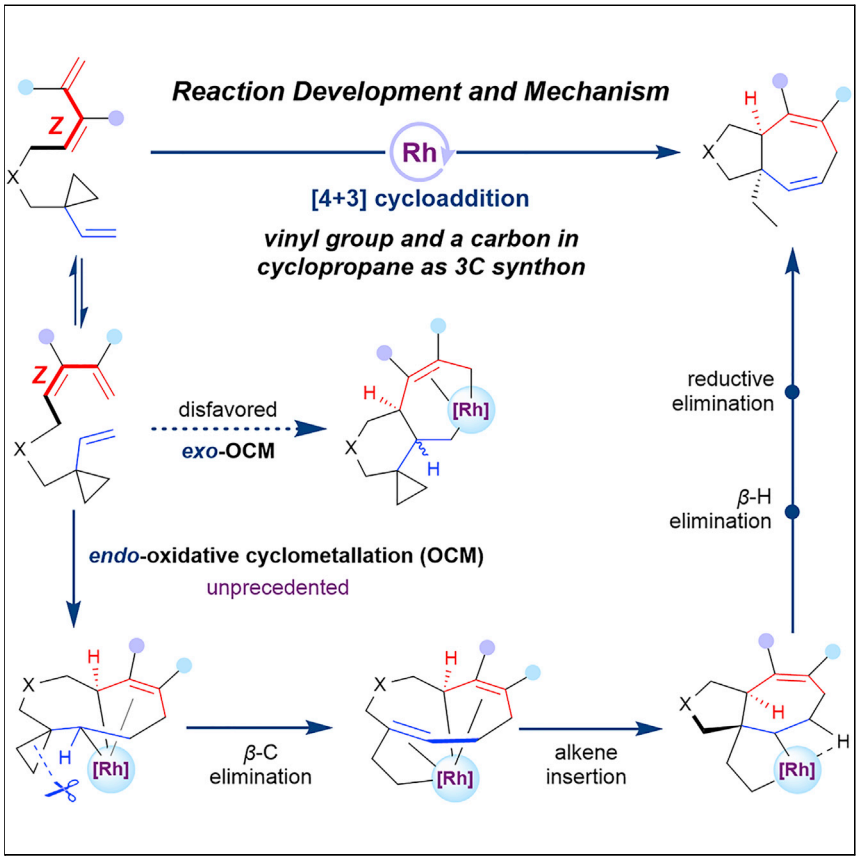

We report here a Rh(I)-catalyzed [4 + 3] cycloaddition of *Z*-diene-vinylcyclopropanes (*Z*-diene-VCPs) to construct challenging 5/7-fused bicyclic rings with a bridgehead all-carbon quaternary center. Detailed quantum chemical calculations and deuterium labeling experiments revealed that an unprecedented *endo*-oxidative cyclometallation (OCM) between the diene and vinyl group in VCP was involved in this [4 + 3] reaction. An understanding of why *endo*-OCM occurs instead of the traditional *exo*-OCM, and factors affecting such selectivity, are provided, which is important for designing new *endo*-OCM embedded reactions catalyzed by transition metals.

Jun Yang, Pan Zhang, Zeyuan Shen, Yi Zhou, Zhi-Xiang Yu

yuzx@pku.edu.cn

Highlights

[4 + 3] reaction of *Z*-diene-VCPs to construct 5/7 bicycles

A vinyl group and a carbon in cyclopropane as 3C synthon

Unprecedented *endo*-oxidative cyclometallation

Combined experimental and DFT study of reaction mechanism

Yang et al., Chem 9, 1477–1494
June 8, 2023
https://doi.org/10.1016/j.chempr.2023.01.020

Chem

CellPress

Article

Unprecedented *endo*-oxidative cyclometallation and [4 + 3] cycloaddition of diene-vinylcyclopropanes

Jun Yang,[1,2] Pan Zhang,[1,2] Zeyuan Shen,[1] Yi Zhou,[1] and Zhi-Xiang Yu[1,3,*]

SUMMARY

The traditional *exo*-oxidative cyclometallation (*exo*-OCM) is a key step in transition-metal-catalyzed reactions. Here, for the first time, we propose an *endo*-oxidative cyclometallation (*endo*-OCM) reaction as a new reaction mode. Realization of *endo*-OCM will add a new concept to chemistry and help the future design of *endo*-[m + n], [m + n + o] cycloadditions and other reactions. We report here that *endo*-OCM exists in a newly developed Rh(I)-catalyzed intramolecular [4 + 3] cycloaddition of *Z*-diene-vinylcyclopropanes (*Z*-diene-VCPs), which provide an efficient way to access challenging 5/7-fused bicyclic skeletons with a bridgehead ethyl substituent. In this [4 + 3] reaction, the *Z*-diene serves as a 4-carbon synthon, while the VCP acts as an unprecedented 3-carbon synthon (two carbon from the vinyl group and one carbon from the cyclopropyl group). Quantum chemical calculations have been carried out to analyze factors affecting the competition of *exo*- and *endo*-OCMs, and to understand why [3 + 2] and expected [4 + 3] reactions of *Z*-diene-VCPs do not happen.

INTRODUCTION

Transition-metal-catalyzed [m + n], [m + n + o] (m, n, and o are referred to the carbon synthons such as CO, carbenes, alkenes, alkynes, dienes, vinylcyclopropanes [VCPs], etc.) cycloadditions for the synthesis of carbocycles, have been becoming powerful tools for chemists.[1–9] Figure 1 shows the paradigmatic mechanisms for the traditional [m + n] and [m + n + o] reactions. These reactions usually start from *exo*-oxidative cyclometallation (*exo*-OCM) to form the fused metallacycles with metal in the *exo* part of the formed bicyclic metallacycles, **MC-I**, which can undergo reductive elimination to give [m + n] cycloadducts. If a new component, o, is introduced, then the insertion of this component into the metal–carbon bond in **MC-I**, followed by reductive elimination, can give traditional [m + n + o] products. We labeled the OCM in the traditional cycloadditions as the *exo*-OCM because there is another OCM, referred to here as *endo*-OCM, which could also be involved in the [m + n] cycloadditions (Figure 1A). *Endo*-OCM produces **MC-II** metallacycles (where a similar intermediate from the insertion reaction of diene to M–C bond was reported[10]) with metal in the *endo* position of the formed bicyclic metallacycles, which can deliver the same [m + n] cycloadducts as the traditional cycloadditions, invoking *exo*-OCM processes. But [m + n + o] cycloadditions involving *endo*-OCM would give bridged [m + n + o] cycloadducts (Figure 1A). Therefore, two cycloadditions, *endo*- and *exo*-[m + n + o] cycloadditions, are named to differentiate them (Figure 1A).

To the best of our knowledge, *endo*-OCM has never been proposed or considered in literature, and the *endo*-[m + n + o] cycloadditions have not been reported either.[11]

THE BIGGER PICTURE

Oxidative cyclometallation (OCM) is a very important and fundamental reaction step in transition-metal-catalyzed cycloadditions. But our understanding of this process is largely limited to *exo*-OCM; the discovery of new cyclometallations can potentially inspire the development of various cycloaddition reactions. In our journey of investigating the Rh-catalyzed [4 + 3] cycloaddition of diene-vinylcyclopropanes, we unexpectedly found a new type of OCM, which is named an *endo*-OCM. This unprecedented *endo*-OCM could be applied to create *endo* cycloaddition reactions and other transformations in the future. Quantum chemical calculations were also applied to understand the competition between *exo*- and *endo*-OCMs. In terms of the practical importance, the present [4 + 3] reaction provides an efficient method to synthesize challenging 5/7 bicycles with a bridgehead ethyl substituent.

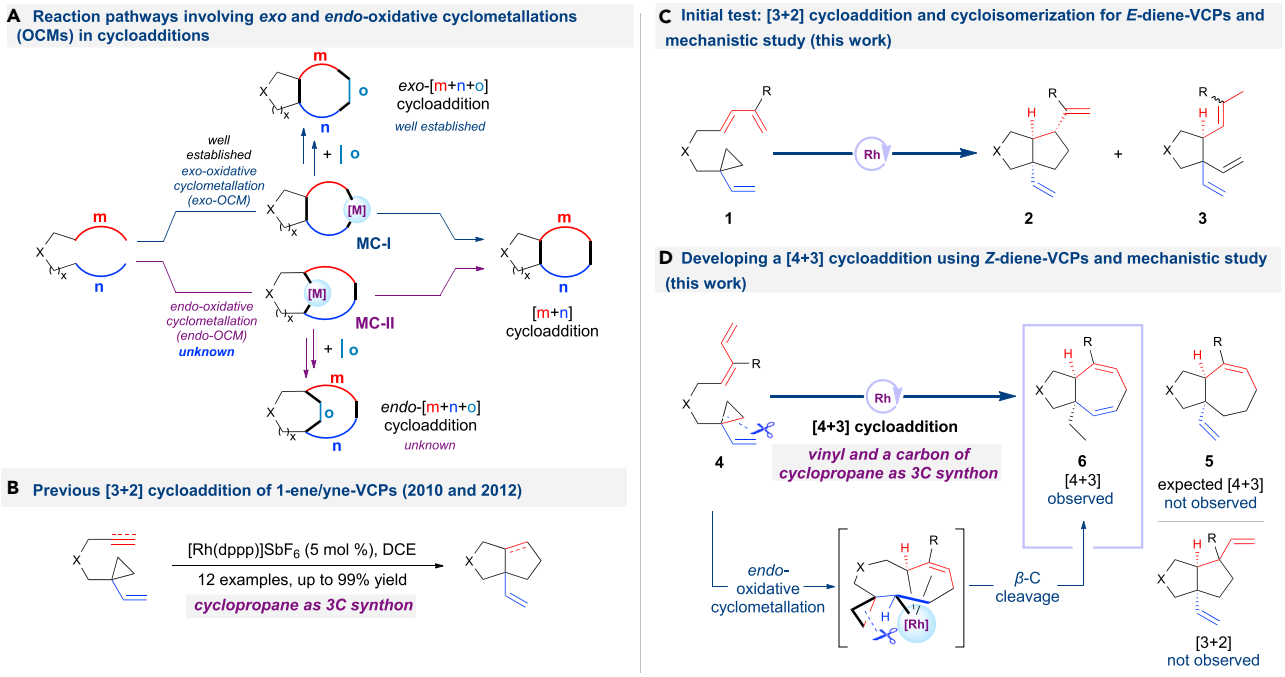

Figure 1. Different types of oxidative cyclometallations (OCMs), previous [3 + 2] cycloaddition of 1-ene/yne-VCPs and new attempts to achieve [4 + 3] cycloaddition of 1-diene-VCPs

(A) Reaction pathways involving *exo* and *endo*-oxidative cyclometallations (OCMs) in cycloadditions.

(B) Previous [3 + 2] cycloaddition of 1-ene/yne-VCPs.

(C) Initial test: [3 + 2] cycloaddition and cycloisomerization for *E*-diene-VCPs and mechanistic study (this work).

(D) Developing a [4 + 3] cycloaddition using *Z*-diene-VCPs and mechanistic study (this work).

Understanding whether *endo*-OCM can occur or not, and the reasons behind this, is important for advancing new concepts and chemistry. Discovery of such OCM in reactions would also be significant, considering that *endo*-[m + n + o] cycloadditions for bridged cycloadducts could then possibly be designed and realized in the future, and many new skeletons from these reactions would then greatly expand the chemical space of functional molecules. Here, we report the discovery of this *endo*-OCM in our journey to develop and understand a [4 + 3] reaction of *Z*-diene-VCPs, which is also presented in this paper (Figure 1D). We have also carried out detailed computational analyses of the factors affecting the competition of *exo*- and *endo*-OCM processes, giving guidance for the future design of *endo*-OCM in the reaction design.

Here, we give a brief background of why and how we developed the present [4 + 3] reaction of *Z*-diene-VCPs, which provides a new way to access challenging 5/7-fused bicyclic systems[1–9,12–22] with a bridgehead ethyl substituent (Figure 1). VCPs, without activating functional groups, have versatile cycloaddition chemistry to build various mono-, bi-, and poly-cyclic ring systems.[23–27] In these reactions, VCPs act as either a 5C or 3C synthon. For example, Wender pioneered [5 + 2] reactions of VCPs with various 2π components.[28] In 2010, our group reported an intramolecular [3 + 2] cycloaddition of 1-ene/yne-VCPs in which VCPs use their cyclopropanes as a 3C synthon and vinyl groups as an indispensable speculator group (Figure 1B).[29–31] Several other reactions using VCPs as a 3C synthon have also been developed by us.[32–34] Based on the [3 + 2] reaction shown in Figure 1B, we were curious to know whether the 2π component in the [3 + 2] reaction could be replaced by a 4π component (such as a diene) so that the corresponding diene-VCPs could give [4 + 3] products, not

[1]Beijing National Laboratory for Molecular Sciences (BNLMS), Key Laboratory of Bioorganic Chemistry and Molecular Engineering of Ministry of Education, College of Chemistry, Peking University, Beijing 100871, China

[2]These authors contributed equally

[3]Lead contact

*Correspondence: yuzx@pku.edu.cn

https://doi.org/10.1016/j.chempr.2023.01.020

[3 + 2] products (Figures 1C and 1D). Our first test of this idea shown in Figure 1C did not succeed because substrates of *E*-diene-VCPs underwent [3 + 2] cycloaddition as the major event, together with a cycloisomerization reaction as the side reaction. We further hypothesized that if the 4π component is a *Z*-diene with a R substituent within, then the corresponding substrates, *Z*-diene-VCPs, could produce the expected [4 + 3] reaction because the *Z* configuration could disfavor the competing [3 + 2] reaction which, at the same time, could also suffer generating a quaternary carbon (Figure 1D). But to our surprise, this reaction gave a 5/7-fused bicyclic ring compound with a bridgehead all-carbon quaternary center[35] (an ethyl rather than a vinyl group in the bridgehead position), and we named this a [4 + 3] reaction, where the vinyl group and a carbon of the cyclopropane acts as a 3C synthon (details will be presented in the following section). This [4 + 3] reaction has good scope and is disclosed in this paper. We then used experimental study and computational calculations to understand why this [4 + 3] reaction, but not the [3 + 2] and expected [4 + 3] reactions, happens, which led us to propose and discover a new mechanism involving *endo*-OCM.

Therefore, in what follows, we will present the whole story of developing the [3 + 2] reaction of *E*-diene-VCPs, designing the [4 + 3] reaction and exploring its reaction scope, studying the mechanism of this [4 + 3] reaction, analyzing the competition of *exo*- and *endo*-OCM processes, and testing experimentally the new theoretical predictions derived from the mechanistic studies here.

RESULTS AND DISCUSSION

[3 + 2] cycloaddition of *E*-diene-VCPs

We initially tested the desired [4 + 3] reaction using *E*-diene-VCP substrate **1a**, finding that no expected [4 + 3] cycloaddition product, but [3 + 2] product together with some side product from β-H elimination, was obtained. After screening reaction conditions (see the supplemental information for details), $[Rh(PPh_3)_3]SbF_6$ was found to be a good catalyst for this transformation. Several other substrates were then studied to get more information of this [3 + 2] reaction (Figure 2). Substrates with a substituent, such as a methyl or an ethyl group, on the position 2 of diene gave good yields together with high selectivity. For substrate **1c** with an *n*-propyl group, both **2c** and **3c** were isolated, with a combined yield of 77%, although low selectivity was observed. Substrate **1d** with an isopropyl group mainly gave **3d**, with **2d** as a minor byproduct (the ratio **2d**:**3d** was 1:8). Oxygen-tethered substrate **1e** can also undergo [3 + 2] cycloaddition with low selectivity and a moderate combined reaction yield. The mechanism of this [3 + 2] reaction, and an understanding of why and how product **3** was generated, are provided in the supplemental information. This reaction has limited synthetic value except for **1a** and **1b** because **1c**–**1e** gave inseparable mixtures.

[4 + 3] cycloaddition of *Z*-diene-VCPs

In order to inhibit [3 + 2] reaction, we tried to use substrates with a substituent in the internal alkene part of the *Z*-diene moiety, namely substrates **4**. In this case, [3 + 2] cycloaddition may be disfavored because it would potentially form a challenging quaternary carbon center in the final products (see Figure 7 for the pathway to ***trans*-2**).[36,37] Due to this, the new substrate may have a greater chance to deliver the expected [4 + 3] product. Another design to help the expected [4 + 3] is using *Z*-dienes, hoping that the geometrical change could also disfavor the [3 + 2] reaction.

We synthesized **4a** with a *Z*-diene and tested its cycloaddition reaction (Figure 3). Under the catalysis of cationic $Rh(PPh_3)_3SbF_6$ in DCE at 80°C, the reaction of **4a**

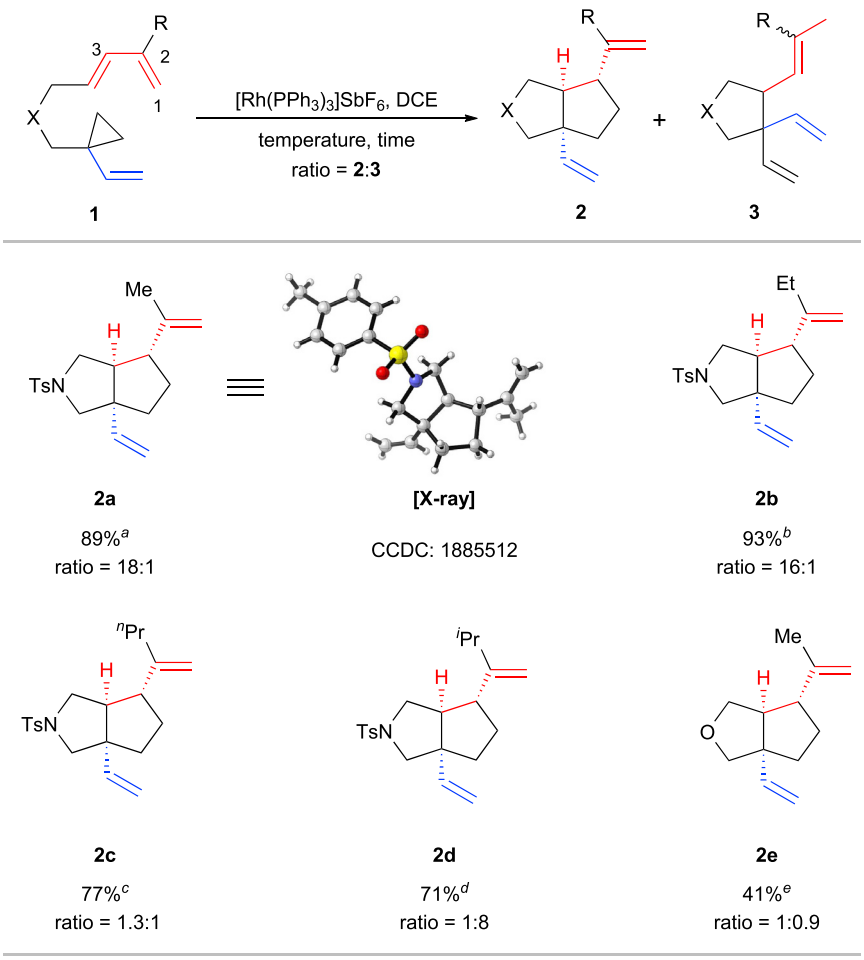

Figure 2. Scope of the [3 + 2] cycloaddition of *E*-diene-VCPs

The above given yields are the average yields of two runs. Ratio = 2:3.

[a]Reaction conditions: $[Rh(PPh_3)_3]SbF_6$ (10 mol %), 0°C, DCE (1,2-dichloroethane), 48 h.

[b]Reaction conditions: $[Rh(PPh_3)_3]SbF_6$ (20 mol %), 0°C, DCE, 48 h.

[c]Reaction conditions: $[Rh(PPh_3)_3]SbF_6$ (20 mol %), 80°C, DCE, 24 h.

[d]Reaction conditions: $[Rh(PPh_3)_3]SbF_6$ (10 mol %), 80°C, DCE, 24 h.

[e]Reaction conditions: $[Rh(PPh_3)_3]SbF_6$ (10 mol %), 80°C, DCE, 22 h.

gave complex mixture (entry 1). We also found that $[Rh(COE)_2Cl]_2$, $[Rh(COD)Cl]_2$ and Wilkinson's catalyst could not catalyze the reaction (entries 2–4). Surprisingly, when $[Rh(CO)_2Cl]_2$ was used as a catalyst in DCE, an unexpected product **6a** with an ethyl group in the bridgehead position was isolated in 60% recovery yield, and the designed [4 + 3] product **5a** with a vinyl group in the bridgehead position was not detected (entry 5). In this [4 + 3] reaction, substrate **4a** used its vinyl group and a carbon in the cyclopropyl group as a 3C synthon, not the originally designed [4 + 3] reaction, where cyclopropane is a 3C synthon and the vinyl group is just a spectator. Substrate **4k** with R=H did not react under the same conditions, implying that R=Me or that other substituents are required for the [4 + 3] reaction (see the bottom of Figure 4). With this exciting and encouraging result, we decided to develop the present [4 + 3] reaction as a general reaction to access a 5/7 ring skeleton.

Further optimization of this [4 + 3] reaction condition is shown in Figure 3. Different solvents were screened, and we found that the isolated yield of **6a** could reach 76%

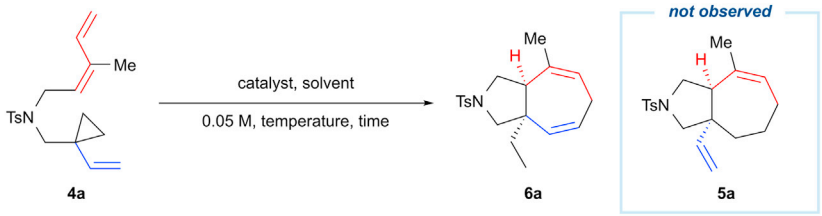

entry	catalyst	temperarure/°C	solvent	time/h	yield[a,b]
1	$[Rh(PPh_3)_3]SbF_6$	80	DCE	2	mixture
2	$[Rh(COE)_2Cl]_2$	80	DCE	9	N. R.
3	$[Rh(COD)Cl]_2$	80	DCE	9	N. R.
4	$Rh(PPh_3)_3Cl$	80	DCE	9	N. R.
5	$[Rh(CO)_2Cl]_2$	90	DCE	48	60%[c]
6	$[Rh(CO)_2Cl]_2$	90	dioxane	4	72%
7	$[Rh(CO)_2Cl]_2$	90	*p*-xylene	12	67%
8	**$[Rh(CO)_2Cl]_2$**	**90**	**PhMe**	**12**	**76%[d]**
9	$[Rh(CO)_2Cl]_2$	80	PhMe	22	65%
10	$[Rh(CO)_2Cl]_2$	100	PhMe	6	75%
11[e]	$[Rh(CO)_2Cl]_2$	100	PhMe	22	68%

Figure 3. Optimization of reaction conditions for [4 + 3] cycloaddition

[a]0.1 mmol substrate and 10 mol % catalyst were used.

[b]Isolated yields.

[c]brsm.

[d]Average yield of two runs.

[e]5 mol % catalyst was used.

when using toluene as a solvent (entry 8). Either lowering the reaction temperature, reducing catalyst loading, or prolonging the reaction time led to a decrease in the reaction yields (entries 9–11). Therefore, the optimal reaction conditions, which will be used in later studies of reaction scope, include using 0.1 mmol scale substrate, 10 mol % $[Rh(CO)_2Cl]_2$ as a catalyst and 2 mL toluene as a solvent under 90°C for 12 h (entry 8, Figure 3).

The scope of this [4 + 3] cycloaddition was then investigated (Figure 4). Under the standard reaction conditions, the reaction yield for substrate **4a** was 76%. For substrates **4b** and **4c** with other alkyl groups, the target cycloadditions occurred smoothly. Substrate **4d**, with a benzyl ether in the diene component, could deliver the [4 + 3] product **6d** in 70% yield. To our delight, substrate **4e** with a phenyl group on diene was tolerated, giving the desired product **6e**. The structure of **6e** was further confirmed by X-ray analysis (CCDC: 2233621). We also evaluated the trisubstituted diene compound **4f**, finding that the [4 + 3] cycloadduct **6f** was generated in 60% yield.

Next, we examined whether substrates with different tethers could be suitable for the [4 + 3] cycloaddition. Both NNs- (4-nitrobenzenesulfonamide) and NBs (4-bromobenzenesulfonamide)-tethered substrates **4g** and **4h** can undergo [4 + 3] reactions without difficulty to give **6g** and **6h**, respectively. We also found that *O*-

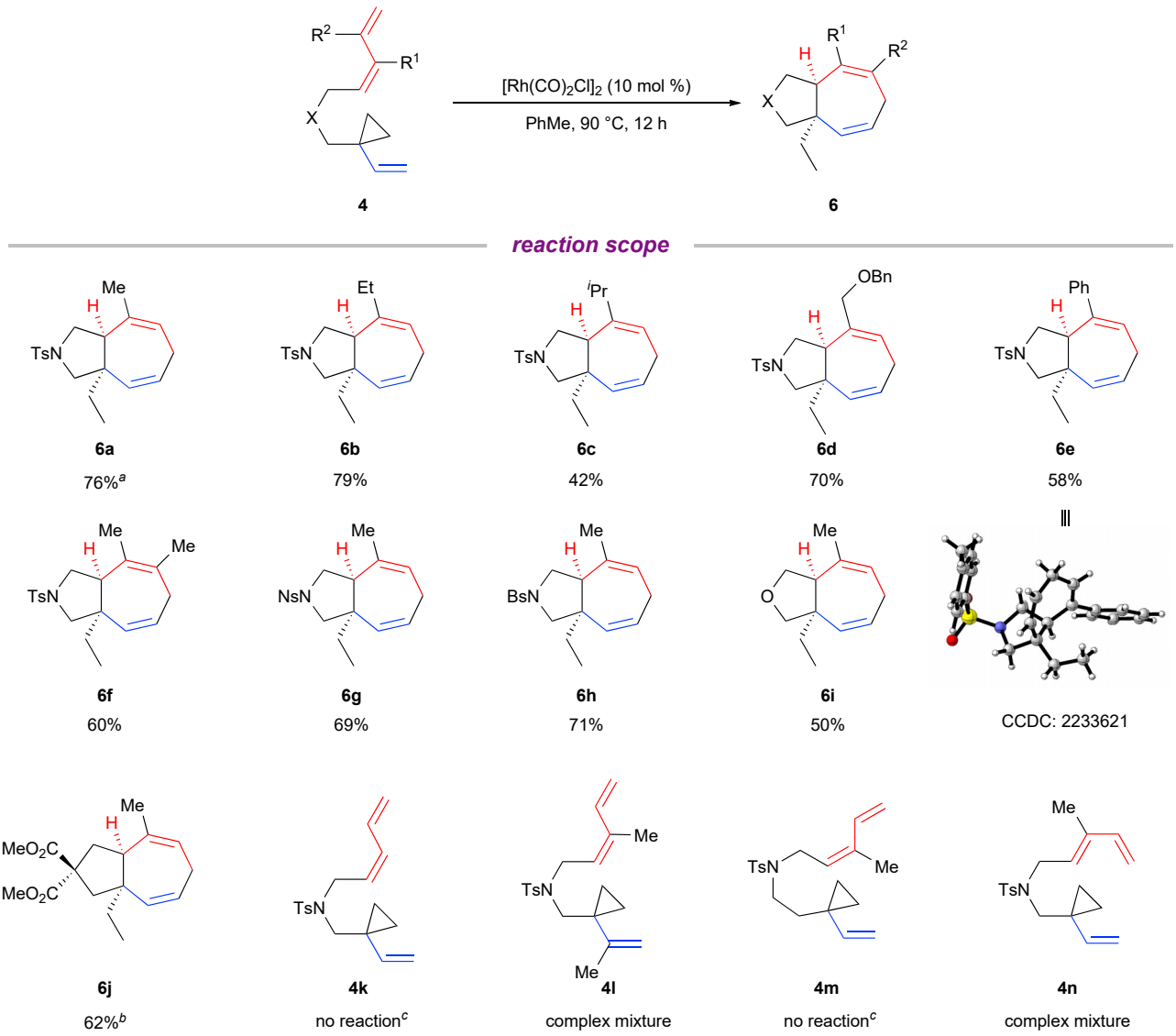

Figure 4. Scope of the [4 + 3] cycloaddition of *Z*-diene-VCPs

The reaction was performed in a 0.1 mmol scale and 2 mL PhMe was used. The yield for each substrate is the average yield of two runs.

[a]Reaction **4a** gave two byproducts from CO (catalyst) insertion (see the supplemental information), which will be reported in the future.

[b]An inseparable, unidentified compound was mixed.

[c]Complex mixture was obtained at elevated temperature (120 °C) in *p*-xylene.

tethered substrate **4i** smoothly delivered [4 + 3] product **6i** in 50% yield. To our delight, treating *C*-tethered substrate **4j** under optimal reaction conditions gave the desired product **6j** in 62% yield, together with a trace amount of inseparable impurity.

As mentioned above, substrate **4k** without a substituent in the diene part could not react. DFT calculations were used to rationalize why substituents were so significant to [4 + 3] cycloadditions, finding that such substituents could accelerate the *endo*-OCM process (see later discussion and the supplemental information). Substrate **4l**, with a methyl group on the VCP, gave an unidentified complex mixture, and substrate **4m**, containing a longer tether with respect to substrate **4a**, stayed intact

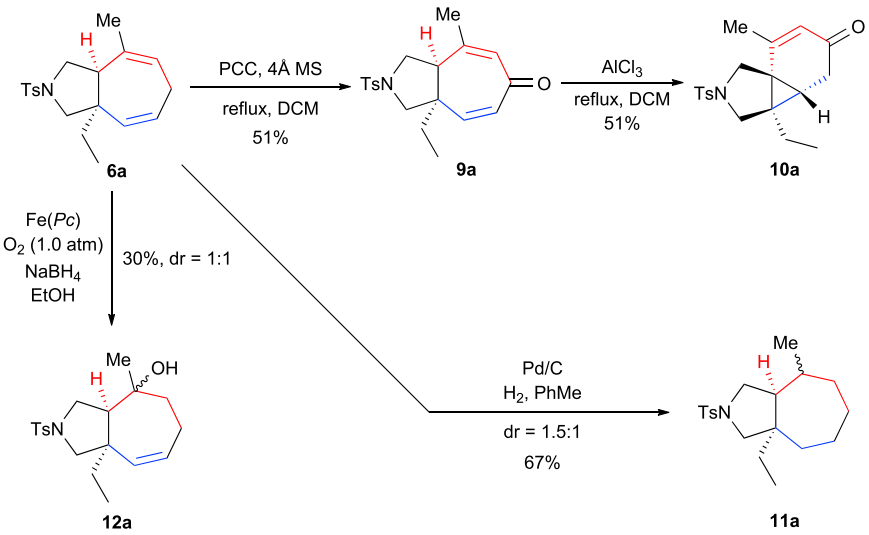

Figure 5. Synthetic applications of the [4 + 3] cycloadduct
The yield for each reaction is the average yield of two runs.

under the optimal reaction conditions. We also synthesized substrate **4n**, which has an *E*-diene, to examine the conformational effects of diene in this [4 + 3] cycloaddition. Unfortunately, the reaction of **4n** delivered a complex mixture, suggesting again that internal alkene with a *Z* configuration in the diene of the diene-VCPs substrates is critical to the success of the present [4 + 3] reaction. We point out here that the present [4 + 3] reaction could have side reactions, such as CO (from the used catalyst) insertion, resulting in minor products. During the study of the present [4 + 3] reaction, we did not check substrates—with the exception of **1a**—and planned to investigate the cycloadditions of all substrates with CO in the future (see the supplemental information).

To further illustrate the synthetic applications of the reaction, we tried to transform the cycloadduct using different reactions (Figure 5). Allylic C–H oxidation of **6a** can be successfully realized by using pyridinium chlorochromate (PCC) as an oxidant, giving **9a** in 51% yield. Interestingly, **9a** can be transformed into a 5/3/6 fused tricycle product **10a** via $AlCl_3$ mediated reaction (possibly via deprotonation/6π pericyclic reaction/protonation) in a yield of 51%. Besides, hydrogenation of **6a** afforded **11a** in a moderate yield. Fe(*Pc*)-mediated oxidation[38] was also tried and we found that the reaction selectively occurred at the electron-rich double bond, giving **12a** in 30% yield.

Mechanism of the [4 + 3] reaction and discovery of *endo*-OCM

To understand the reaction mechanism more deeply, both experiments and quantum chemical calculations were conducted. For experimental mechanistic study, visual kinetic analysis[39,40] was carried out to illustrate reaction orders in the substrate and catalyst. Then, quantum chemical calculations were applied to provide detailed reaction pathways.

Visual kinetic analysis

We monitored the reaction of **4a** by ^{1}H NMR spectroscopy and analyzed the data by a normalized timescale[39] method and variable time normalization analysis.[40] Considering that there are two CO insertion byproducts generated in the early stage (see

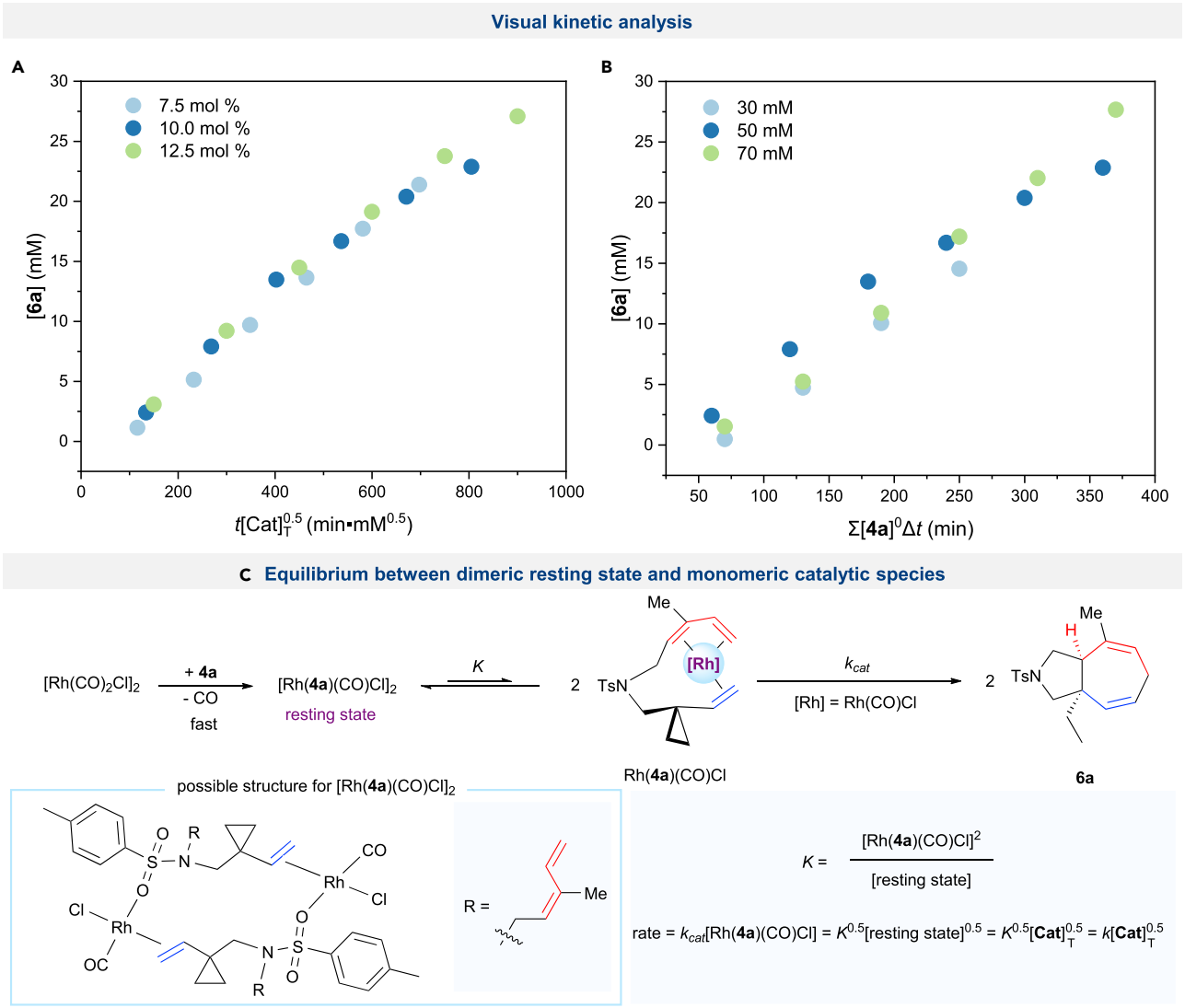

Figure 6. Visual kinetic analysis on substrate 4a and equilibrium between dimeric resting state and monomeric catalytic species

(A and B) Reaction conditions: (A) **4a** (50 mM), $[Rh(CO)_2Cl]_2$ (7.5, 10.0, 12.5 mol %), 90°C; (B) **4a** (30, 50, 70 mM), $[Rh(CO)_2Cl]_2$ (5 mM), 90°C. $[Cat]_T$ is the total concentration of catalyst added.

(C) Equilibrium between dimeric resting state and monomeric catalytic species.

supplemental information for details), the kinetic data were collected after the reaction was run for 1 h. The order in $[Rh(CO)_2Cl]_2$ for the [4 + 3] cycloaddition was found to be 0.5 (Figure 6A). While, to our surprise, the reaction is zero order in **4a** (Figure 6B). The 0.5 order in the catalyst implies that the resting state is dimeric and that there is an equilibrium between the resting state ($[Rh(\mathbf{4a})(CO)Cl]_2$, a possible structure has been proposed in Figure 6C based on similar structures reported in Le Gall et al.[41]) and the active catalytic species (Rh(**4a**)(CO)Cl). The zero order in the substrate suggests that two substrates are involved in the resting state (Figure 6C).

Disfavored pathway A involving oxidative addition of VCPs

DFT studies were further applied to elucidate mechanistic details of the [4 + 3] reaction. Pathway A (Figure 7) was originally proposed to account for the mechanism of [4 + 3] cycloaddition.

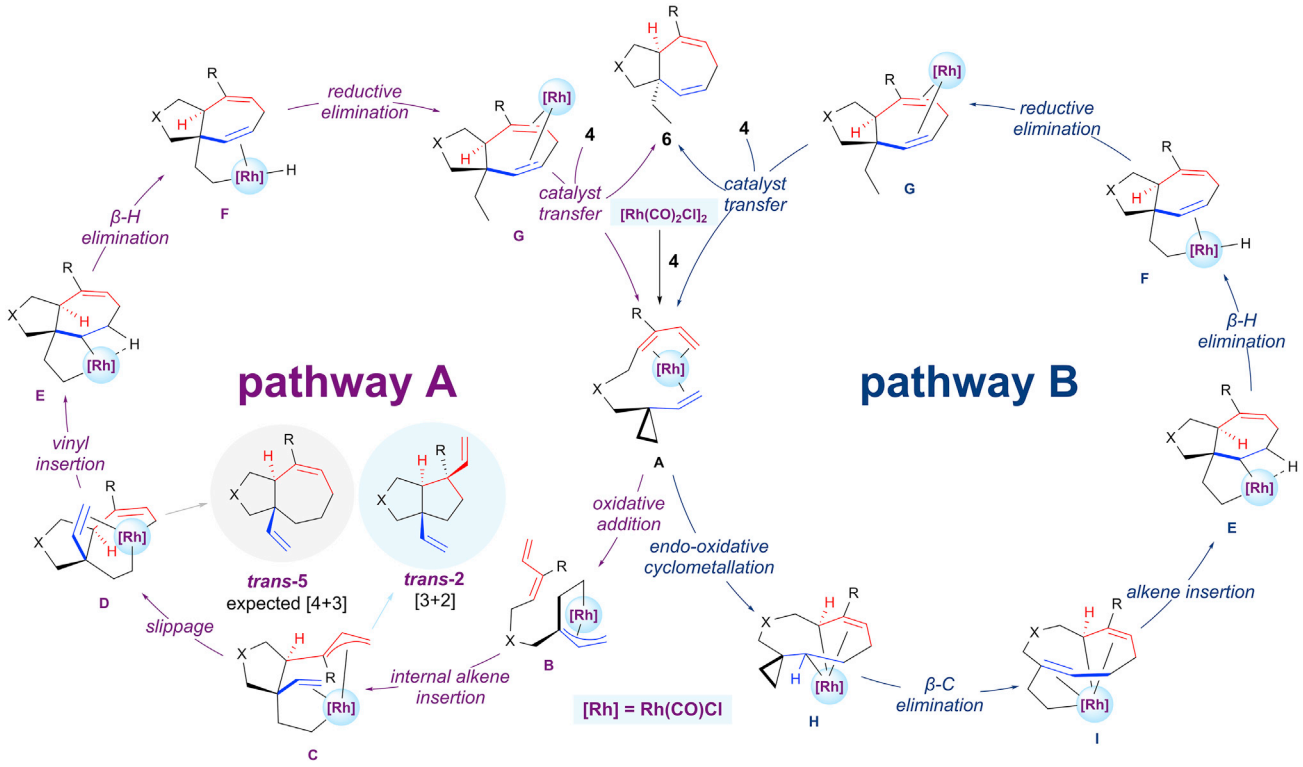

Figure 7. Proposed pathways A and B of the [4 + 3] cycloaddition of *Z*-diene-VCPs

In pathway A, shown in Figure 7, complexation of the substrate with the catalyst (via ligand exchange between product-catalyst complex **G** and substrate **4**) affords **A**, which undergoes the oxidative addition of cyclopropane to produce intermediate **B**. Subsequent insertion of diene's internal alkene into the C–Rh bond produces **C**. After that, **C** turns into **D** via allylic slippage. If reductive elimination from **D** is favored, the expected [4 + 3] reaction would take place to give product ***trans*-5**. This expected [4 + 3] cycloaddition was not observed experimentally, suggesting that insertion of the bridgehead vinyl group into the C–Rh bond may be preferred to generate **E**, which then undergoes β-hydride elimination and reductive elimination to give the final [4 + 3] cycloadduct **6**.

DFT calculations[42] were carried out at SMD(toluene)/BMK/def2-TZVPP//BMK/6-31G(d)/LANL2DZ level[43–47] (see supplemental information for details) by using *O*-tethered **4i** as a model substrate (Figure 8). BMK was used because it was tested and found to be excellent in computing $[Rh(CO)_2Cl]_2$ catalyzed cycloadditions according to our recent benchmark study.[48] However, DFT studies excluded pathway A because intermediate **C** in this pathway favors giving the [3 + 2] cycloaddition product instead of the [4 + 3] product. Here, we briefly describe why this pathway is not preferred. Figure 8A shows that in pathway A the reaction starts with an oxidative addition of VCP with an activation free energy of 9.1 kcal/mol via **TS1**. Then, the proximal double bond of the diene moiety coordinates with the Rh center to generate **IN3**, which then undergoes *trans* alkene insertion via transition state **TS2** to deliver **IN4** (*trans*-cycloaddition; here, the prefix *trans* means that the bridgehead hydrogen atom and vinyl group are in the *trans* position after cycloaddition). This step requires an activation energy of 29.6 kcal/mol (from **IN2** to **TS2**). The alkene insertion could also give a *cis* intermediate **IN4-*cis*** (*cis*-cycloaddition; here, prefix *cis* means that the bridgehead hydrogen atom and vinyl group are in the *cis*

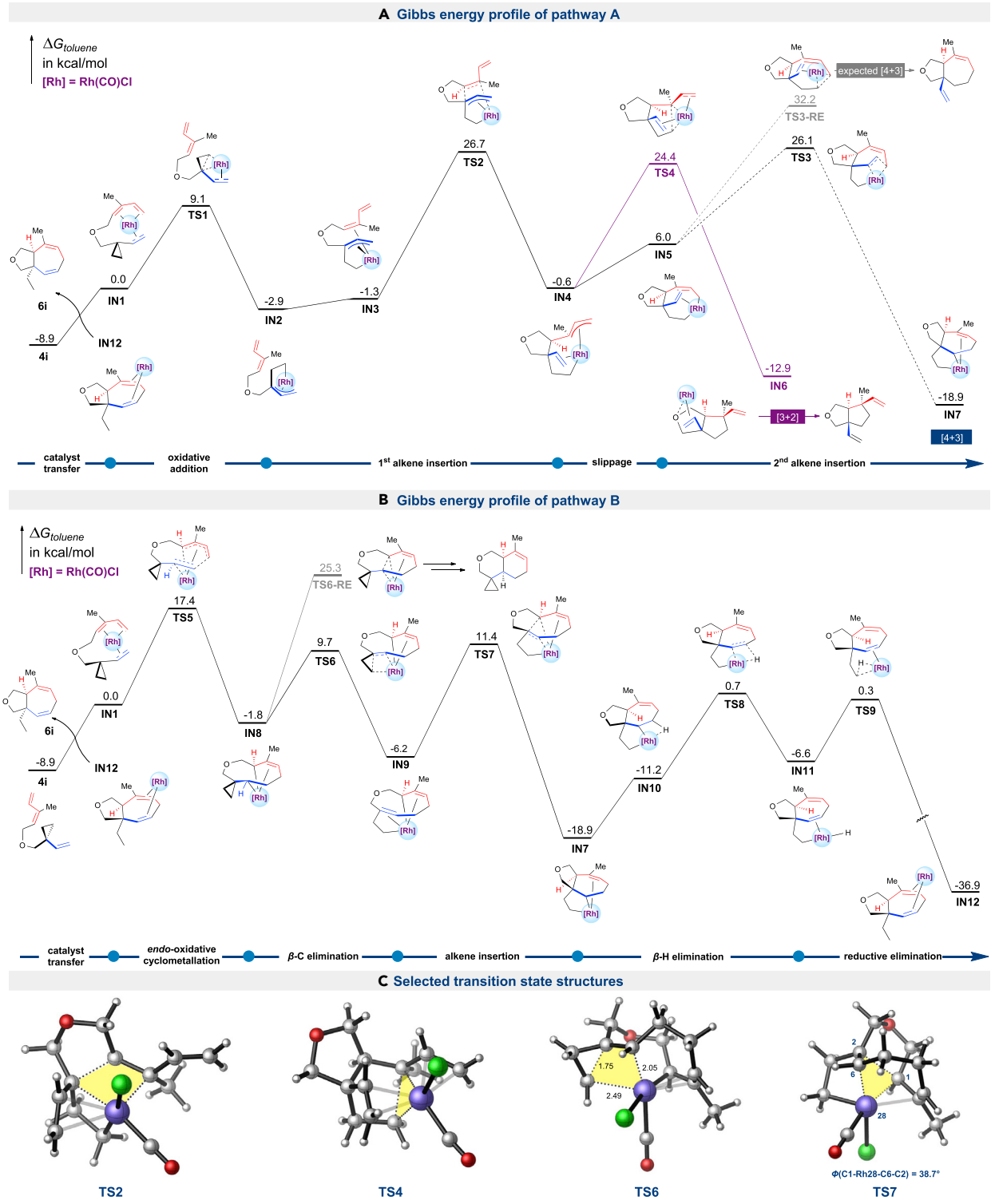

Figure 8. Gibbs energy profiles and selected transition state structures for pathways A and B of the [4 + 3] reaction of *Z*-diene-VCP

Computed at the SMD(toluene)/BMK/def2-TZVPP//BMK/6-31G(d)/LANL2DZ level. Color scheme: H, white; C, gray; O, red; Cl, green; Rh, violet. Bond lengths are reported in Å.

(A) Gibbs energy profile of pathway A.

(B) Gibbs energy profile of pathway B.

(C) Selected transition state structures.

position after cycloaddition), which can be excluded for further consideration due to the high barriers (details are given in supplemental information).

IN4 has three transformation pathways. One is to form [3 + 2] product via **TS4** to give **IN6**. Alternatively, **IN4** isomerizes to η^1-coordinated intermediate **IN5**, which then undergoes either the expected [4 + 3] pathway via **TS3-RE**, or vinyl insertion into the C–Rh bond to give **IN7**. After that, **IN7** undergoes further transformations to give the final [4 + 3] product. These three pathways have their respective transition states, **TS4** (24.4 kcal/mol), **TS3-RE** (32.2 kcal/mol), and **TS3** (26.1 kcal/mol), among which **TS4** is more favorable. This suggests that the *trans*-cycloaddition pathway is preferred and gives [3 + 2] product instead of the expected [4 + 3] or [4 + 3] product. This result was in contrast to the experimental observation. Besides, *cis*-cycloaddition of pathway A is also predicted to give other products instead of what is observed experimentally (see supplemental information). Consequently, a new mechanism, which is pathway B involving *endo*-OCM, is needed to account for the experimental observations. This is presented in Figure 8B.

Computational understanding of the competition between exo- and endo-OCMs in Rh-catalyzed intramolecular [4 + 2] cycloaddition of butadiene and alkenes

Before we discuss pathway B, we first discuss *exo*- and *endo*-OCMs in Rh-catalyzed intramolecular [4 + 2] cycloadditions[49–52] between dienes and alkenes. These [4 + 2] reactions can be divided into four catalogs, namely E5/6, E6/6, Z5/6, and Z6/6, where E and Z represent an *E*-diene or a *Z*-diene, while 5/6 and 6/6 indicate that the generated bicyclic products are 5/6 or 6/6 bicycle skeletons. The 5/6 and 6/6 products could have *cis* or *trans* configurations, but here we only present the kinetically favored ones suggested from *ab initio* calculations.

All the four catalogs of [4 + 2] reactions could take place either via *exo*- or *endo*-OCM, followed by reductive elimination to deliver the final cycloadducts (Figure 9A). In the *exo*-OCM transition states containing 7-membered rhodacycles of diene, alkene, and Rh, which are labeled T rings (T, traditional), are forming. While in *endo*-OCMs, two metallacycles are forming, the left one is labeled an L ring (by the tether and Rh), and the other is an R ring (by Rh, diene, and alkene). Here, L means left and R means right. State-of-the-art DLPNO-CCSD(T)[53–56] calculations were applied to investigate the kinetic preferences of these OCMs.

For E5/6, *exo*-OCM is favored kinetically by 15.0 kcal/mol compared with *endo*-OCM because the latter suffers from generating a highly strained 6-membered L ring and a 7-membered R ring. But for the Z5/6 system, this kinetic energy preference of *exo*- compared with *endo*-OCM is reduced to 10 kcal/mol because the *Z*-diene introduces the repulsion of metal and the tether, caused by the geometry of the diene in the *exo*-OCM transition state. Therefore, for E5/6 and Z5/6 catalogs, *endo*-OCMs are impossible.

In the E6/6 catalog, *exo*-OCM is only 2.9 kcal/mol favored kinetically over *endo*-OCM in that the forming L ring in the *endo*-OCM transition state is a 7-membered metallacycle (consisting of the 6-atom tether and Rh) and this bigger ring experiences less congestion. To our delight, in the Z6/6 catalog, *exo*- and *endo*-OCMs now have almost the same activation free energies. This is due to a trade-off: in the *endo*-OCM transition state, the forming L ring is a 7-membered metallacycle consisting of the 6-atom tether and Rh, with small ring strain; while the *exo*-OCM transition state is punished by the T ring distortion caused by the *Z*-diene geometry. Detailed analysis of ring strains is given in supplemental information.

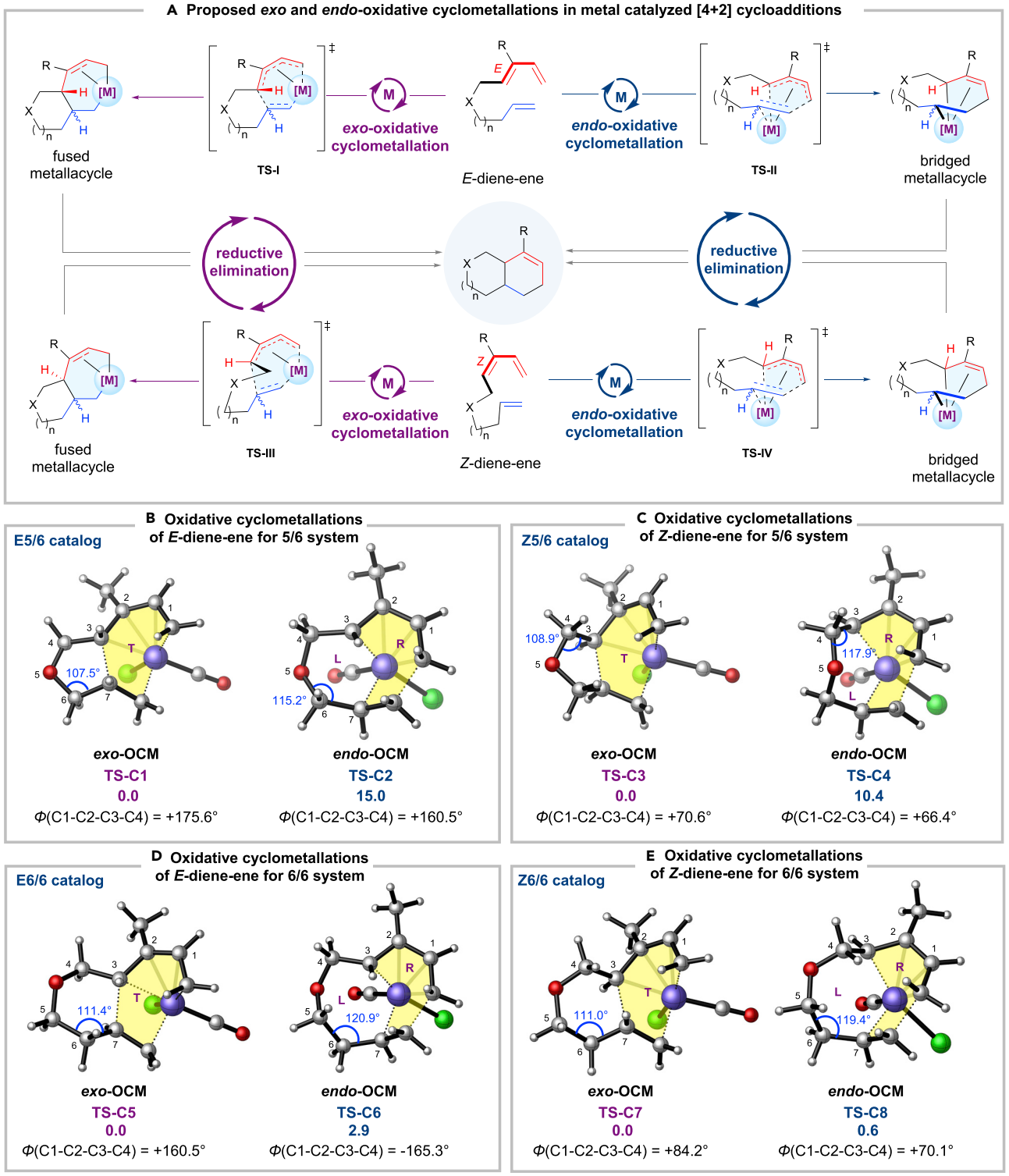

Figure 9. *Exo*- and *endo*-ene/diene oxidative cyclometallations (OCMs)

Relative Gibbs energies are reported in kcal/mol, computed at SMD(toluene)/DLPNO-CCSD(T)/def2-TZVPP//BMK/6-31G(d)/LANL2DZ level. Color scheme: H, white; C, gray; O, red; Cl, green; Rh, violet. T, traditional; L, left; R, right.

(A) Proposed *exo* and *endo*-oxidative cyclometallations in metal catalyzed [4 + 2] cycloadditions.

(B) Oxidative cyclometallations of *E*-diene-ene for 5/6 system.

Figure 9. *Continued*
(C) Oxidative cyclometallations of *Z*-diene-ene for 5/6 system.
(D) Oxidative cyclometallations of *E*-diene-ene for 6/6 system.
(E) Oxidative cyclometallations of *Z*-diene-ene for 6/6 system.

The above analysis suggests that, to favor *endo*-OCM, the tether between diene and alkene must be longer; for example, a 6-atom tether is preferred so that the L rings in the transition states experience less ring strains.[10] On the other hand, using *Z*-dienes to make *exo*-OCMs creates repulsion between the tether and the Rh in forming the R rings. These insights are useful and can be helpful for the future design of *endo*-[m + n] and *endo*-[m + n + o] cycloadditions with *endo*-OCMs.

Favored pathway B involving endo-OCM

The above analysis indicates that the *endo*-OCM may occur for *Z*-diene-VCP, which is involved in pathway B (Figure 7). In pathway B, substrate-catalyst complex **A** first undergoes *endo*-ene/diene OCM (forming a bridged metallacycle) to give **H**. Then β-C cleavage of the cyclopropane takes place to give intermediate **I**, which is then converted to **E** via alkene insertion. After that, the steps followed are the same as those in pathway A.

As shown in Figure 8B, in pathway B, an irreversible *endo*-OCM of **IN1** via **TS5** affords a unique Rh-bridged spiro[2.9]dodecane heterocycle **IN8**, which needs an activation free energy of 17.4 kcal/mol. After **IN8** is formed, β C–C bond cleavage of cyclopropane takes place through **TS6** to give **IN9**. This process has an activation free energy of only 11.5 kcal/mol. **TS6** is an early transition state and the energy needed for β C–C bond cleavage is not high. This can be understood by checking the structure of **TS6**, in which the distance of the broken C–C bond of cyclopropane is only 1.75 Å and the newly forming Rh–C bond is 2.49 Å.

We then proposed a new alkene insertion process: the newly formed alkene moiety in **IN9** inserts into the Rh–C bond of this intermediate, giving **IN7** (via **TS7**), which requires 17.6 kcal/mol of activation free energy and is exergonic by 12.7 kcal/mol. Subsequently, isomerization of **IN7** gives **IN10**, which then undergoes β-H elimination to afford the Rh–H species **IN11** via **TS8**. An easy reductive elimination then takes place to generate the product-coordinated Rh complex **IN12**. Finally, **IN12** undergoes a ligand exchange reaction with the substrate to liberate the [4 + 3] product and **IN1**, which can then join the next catalytic cycle. In addition, our calculations found that **IN9** could also undergo reductive elimination. Unfortunately, this process is much disfavored because a strained bridged bicycle would be formed in this pathway (see supplemental information).

The most difficult step in pathway A is the 1st alkene insertion via **TS2**, while the *endo*-OCM via **TS5** is the most difficult step in pathway B. **TS2** in pathway A is 9.3 kcal/mol higher than **TS5** in pathway B in terms of Gibbs free energy, suggesting that pathway B is much more favored. Therefore, [4 + 3] product is preferentially generated, consistent with the experimental observation.

Why pathway B is favored over pathway A? We attribute this to the formation of a larger and more stable rhodacycle via *endo*-OCM. Besides, the β C–C bond cleavage of cyclopropane is easy. In contrast, the alkene insertion via **TS2** in pathway A is difficult, considering that the insertion alkene is trisubstituted while our previous successful [3 + 2] reaction only used terminal akenes.[29–31]

Here, we must point out that even though pathway B is favored, the reaction of *Z*-diene-VCPs in the reaction process first undergoes cyclopropane cleavage, forming **IN2** via

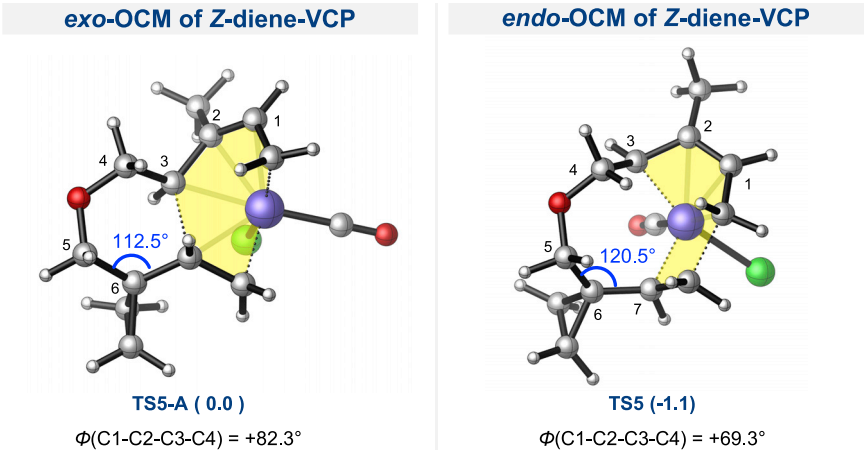

Figure 10. Comparison of *exo*- and *endo*-OCM transition state structures for *Z*-diene-VCP
Computed at SMD(toluene)/DLPNO-CCSD(T)/def2-TZVPP//BMK/6-31G(d)/LANL2DZ level. Color scheme: H, white; C, gray; O, red; Cl, green; Rh, violet.

pathway A because this is favored. Then **IN2** will not continue pathway A (passing **TS2** of alkene insertion in this pathway is difficult) but go back to form the substrate again, which then enters pathway B to give the final [4 + 3] product, based on the Curtin-Hammett principle.

Why not [4 + 2] reaction for Z-diene-VCPs?

All substrates of *Z*-diene-VCPs could possibly form [4 + 2] product via either *exo*- and *endo*-OCMs. As mentioned above, the reductive elimination from **IN8** is disfavored by 15.6 kcal/mol and no [4 + 2] product could be generated by this pathway involving *endo*-OCM (Figure 8B). Here, we show that generating [4 + 2] product from *exo*-OCM is also disfavored because DFT calculations show that *exo*-OCM via **TS5-A** is higher than **TS5** by 1.1 kcal/mol (Figure 10). The energy difference may be underestimated because no [4 + 2] product was observed experimentally. This can be well understood by using the rationalization shown in section computational understanding of the competition between *exo*- and *endo*-OCMs in Rh-catalyzed intramolecular [4 + 2] cycloaddition of butadiene and alkenes.

Deuterium labeling experiment and designed experiment supporting E-diene-VCPs giving [4 + 2] product

To further support our calculations, we carried out the deuterium labeling experiment by using **4a-D** as the substrate. As expected, one deuterium atom on the vinyl group transferred to the 7-membered ring (in **6a-D**), which means the vinyl and a carbon of the cyclopropane act as an untraditional 3-carbon synthon.

The above mechanistic insights also indicate that *E*-diene-VCPs belonging to E6/6 catalog favors *exo*-OCM. We then hypothesized that such substrates could give [4 + 2] products if the reductive elimination followed is preferred over the competing steps in both pathways A and B. Unfortunately, substrate **4n** with an *E*-diene moiety gave a complex mixture under the standard conditions ($[Rh(CO)_2Cl]_2$ as catalyst) and we were not sure whether there were [4 + 2] cycloadducts in the mixture. Then, we decided to synthesize a new substrate **4o** with an *E*-type diene (with a Ph group within) to test our prediction (it should be noted that **4o** is a *Z*-diene-VCP according to the nomenclature rules, while here we still name it an *E*-diene-VCP because it has the same substitution pattern as other *E*-diene-VCPs).

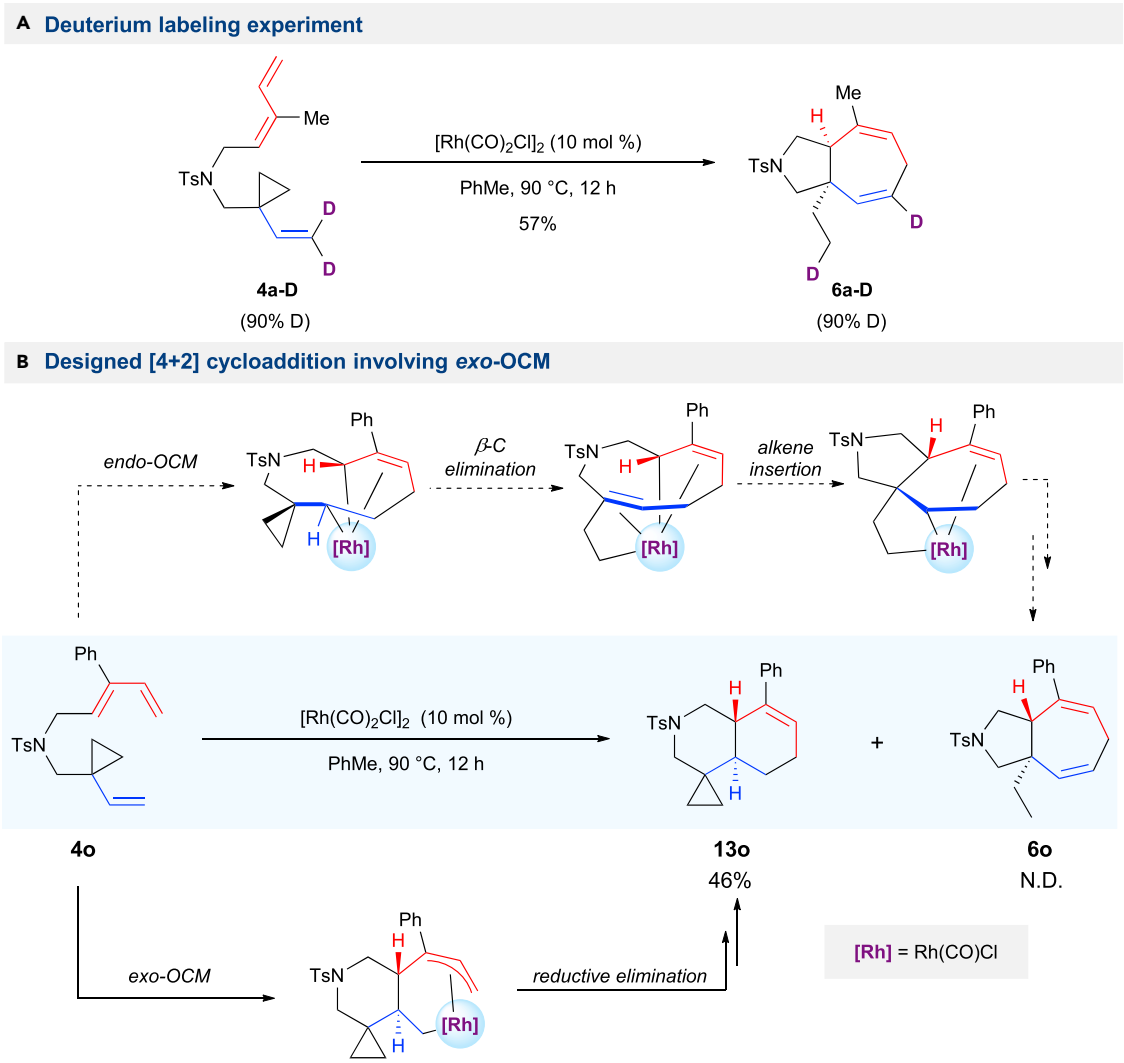

Figure 11. Deuterium labeling experiment and [4 + 2] cycloaddition of *E*-diene-VCP 4o

(A) Deuterium labeling experiment.

(B) Designed [4 + 2] cycloaddition involving *exo*-OCM.

To our delight, under the standard conditions, **4o** gave a [4 + 2] cycloaddition product **13o** with an isolated yield of 46% and no [4 + 3] product was observed (Figure 11), which supports our intuition gained from the above *ab initio* calculations. To further understand the selectivity, DFT calculations were also applied (see supplemental information for details). The major reason for this substrate choosing the [4 + 2] reaction is that pathway B, involving *endo*-OCM, would produce **6o** with a *trans*-5/7 skeleton, which is energetically disfavored (Figure 11, the Rh and the bridgehead H in these intermediates are in *trans* configuration). While using substrates with *Z*-dienes, the 5/7 products formed are in *cis* configuration and pathway B is favored over [4 + 2]. This new experiment and calculations give further support to pathway B for the *Z*-diene-VCPs' [4 + 3] reaction, discussed in this paper.

Conclusions

In summary, an unexpected Rh(I)-catalyzed [4 + 3] cycloaddition of *Z*-diene-VCPs has been developed to construct challenging 5/7-fused bicyclic rings with a bridgehead all-carbon quaternary center. In this [4 + 3] reaction, the VCPs in the substrates serve

as unprecedent three-carbon synthons by using its vinyl group and one carbon of the cyclopropyl group, and the diene moiety in the substrates must be in a *Z* configuration. Detailed DFT calculations and D-labeling experiments have been performed to understand how the [4 + 3] reaction takes place and why the expected [4 + 3] reaction is disfavored, revealing that an unprecedented *endo*-OCM between the diene and vinyl group of VCP was key to the realization of the present cycloaddition. Insights about competition of *exo*- and *endo*-OCMs have been obtained through calculations and new experiments. Discovery of this novel *endo*-OCM of dienes and alkenes is important for inspiring chemists to achieve new metal-catalyzed cycloaddition reactions, especially the *endo*-[m + n + o] cycloadditions.

EXPERIMENTAL PROCEDURES

Resource availability

Lead contact

Further information and requests for resources should be directed to and will be fulfilled by the lead contact, Zhi-Xiang Yu (yuzx@pku.edu.cn).

Materials availability

All materials generated in this study are available from the lead contact without restriction.

Data and code availability

The accession numbers for the **2a** and **6e** reported in this paper are CCDC: 1885512, 2233621, respectively.

SUPPLEMENTAL INFORMATION

Supplemental information can be found online at https://doi.org/10.1016/j.chempr.2023.01.020.

ACKNOWLEDGMENTS

We thank the National Natural Science Foundation of China (21933003) for financial support. We also thank Dr Jie Su for X-ray crystal analysis and the High-Performance Computing Plat-form of Peking University for providing computational resources.

AUTHOR CONTRIBUTIONS

J.Y., P.Z., Z.S., and Y.Z. conducted the experiments and computations. J.Y., P.Z., Z.S., Y.Z., and Z.-X.Y. designed the experiments and wrote the paper. Z.-X.Y. designed and supervised the project.

DECLARATION OF INTERESTS

The authors declare no competing interests.

Received: May 20, 2022
Revised: December 7, 2022
Accepted: January 28, 2023
Published: February 22, 2023

REFERENCES

1. Lautens, M., Klute, W., and Tam, W. (1996). Transition metal-mediated cycloaddition reactions. Chem. Rev. *96*, 49–92. https://doi.org/10.1021/cr950016l.

2. Ojima, I., Tzamarioudaki, M., Li, Z., and Donovan, R.J. (1996). Transition metal-catalyzed carbocyclizations in organic synthesis. Chem. Rev. *96*, 635–662. https://doi.org/10.1021/cr950065y.

3. Gibson, S.E., and Stevenazzi, A. (2003). The Pauson–Khand reaction: the catalytic age Is here! Angew. Chem. Int. Ed. Engl. *42*, 1800–1810. https://doi.org/10.1002/anie.200200547.

4. Kitagaki, S., Inagaki, F., and Mukai, C. (2014). [2+2+1] cyclization of allenes. Chem. Soc. Rev. *43*, 2956–2978. https://doi.org/10.1039/C3CS60382B.

5. Aubert, C., Fensterbank, L., Garcia, P., Malacria, M., and Simonneau, A. (2011). Transition metal catalyzed cycloisomerizations of 1,n-allenynes and -allenenes. Chem. Rev. *111*, 1954–1993. https://doi.org/10.1021/cr100376w.

6. Hartley, R.C., and Caldwell, S.T. (2000). Novel methods for the synthesis of three-, four-, five-, six- and seven-membered, saturated and partially unsaturated carbocycles. J. Chem. Soc. Perkin Trans. 1 *4*, 477–501. https://doi.org/10.1039/A804421J.

7. Yu, Z.X., Wang, Y., and Wang, Y. (2010). Transition-metal-catalyzed cycloadditions for the synthesis of eight-membered carbocycles. Chem. Asian J. *5*, 1072–1088. https://doi.org/10.1002/asia.200900712.

8. Wang, Y., and Yu, Z.-X. (2015). Rhodium-catalyzed [5 + 2 + 1] cycloaddition of ene-vinylcyclopropanes and CO: reaction design, development, application in natural product synthesis, and inspiration for developing new reactions for synthesis of eight membered carbocycles. Acc. Chem. Res. *48*, 2288–2296. https://doi.org/10.1021/acs.accounts.5b00037.

9. Wang, L.-N., and Yu, Z.-X. (2020). Transition-metal-catalyzed cycloadditions for the synthesis of eight-membered carbocycles: an update from 2010 to 2020. Chin. J. Org. Chem. *40*, 3536–3558. https://doi.org/10.6023/cjoc202010025.

10. Zhang, J., Wang, X., and Xu, T. (2021). Regioselective activation of benzocyclobutenones and dienamides lead to anti-Bredt bridged-ring systems by a [4+4] cycloaddition. Nat. Commun. *12*, 3022. https://doi.org/10.1038/s41467-021-23344-0.

11. If the tether is very long, the cycloaddition can be regarded as intermolecular process and this does not satisfy our definition of endo-OCM. For example, Krafft reported such Pauson-Khand reaction involving forming a big 11-membered metallacycle, see, Krafft, M.E., Fu, Z., and Boñaga, L.V.R. (2001). Synthesis of medium-sized rings using the intramolecular Pauson–Khand reaction. Tetrahedron Lett. *42*, 1427–1431. https://doi.org/10.1016/S0040-4039(00)02299-1.

12. Kuila, B., Kaur, M., Singh, P., and Bhargava, G. (2018). Transition-metal-catalyzed [3+2+2] cycloaddition reactions. Eur. J. Org. Chem. *2018*, 853–868. https://doi.org/10.1002/ejoc.201701116.

13. Battiste, M.A., Pelphrey, P.M., and Wright, D.L. (2006). The cycloaddition strategy for the synthesis of natural products containing carbocyclic seven-membered rings. Chemistry *12*, 3438–3447. https://doi.org/10.1002/chem.200501083.

14. Yin, Z., He, Y., and Chiu, P. (2018). Application of (4+3) cycloaddition strategies in the synthesis of natural products. Chem. Soc. Rev. *47*, 8881–8924. https://doi.org/10.1039/C8CS00532J.

15. Lam, H., and Lautens, M. (2020). Recent advances in transition-metal-catalyzed (4+3)-cycloadditions. Synthesis *52*, 2427–2449. https://doi.org/10.1055/s-0039-1690875.

16. Trost, B.M., Zuo, Z., and Schultz, J.E. (2020). Transition-metal-catalyzed cycloaddition reactions to access seven-membered rings. Chemistry *26*, 15354–15377. https://doi.org/10.1002/chem.202002713.

17. Pellissier, H. (2018). Recent developments in the [5+2] cycloaddition. Adv. Synth. Catal. *360*, 1551–1583. https://doi.org/10.1002/adsc.201701379.

18. Nguyen, T.V., Hartmann, J.M., and Enders, D. (2013). Recent synthetic strategies to access seven-membered carbocycles in natural product synthesis. Synthesis *45*, 845–873. https://doi.org/10.1055/s-0032-1318152.

19. Trillo, B., López, F., Gulías, M., Castedo, L., and Mascareñas, J.L. (2008). Platinum-catalyzed intramolecular [4c+3c] cycloaddition between dienes and allenes. Angew. Chem. Int. Ed. Engl. *47*, 951–954. https://doi.org/10.1002/anie.200704566.

20. Alonso, I., Faustino, H., López, F., and Mascareñas, J.L. (2011). Enantioselective gold(I)-catalyzed intramolecular (4+3) cycloadditions of allenedienes. Angew. Chem. Int. Ed. Engl. *50*, 11496–11500. https://doi.org/10.1002/anie.201105815.

21. Shu, D., Song, W., Li, X., and Tang, W. (2013). Rhodium- and platinum-catalyzed [4+3] cycloaddition with concomitant indole annulation: synthesis of cyclohepta[*b*]indoles. Angew. Chem. Int. Ed. Engl. *52*, 3237–3240. https://doi.org/10.1002/anie.201209266.

22. Gulías, M., Durán, J., López, F., Castedo, L., and Mascareñas, J.L. (2007). Palladium-catalyzed [4 + 3] intramolecular cycloaddition of alkylidenecyclopropanes and dienes. J. Am. Chem. Soc. *129*, 11026–11027. https://doi.org/10.1021/ja0756467.

23. Fan, X., Liu, C.-H., and Yu, Z.-X. (2019). Rhodium(I)-catalyzed cycloadditions involving vinylcyclopropanes and their derivatives. In Rhodium catalysis in sorganic synthesis: methods and reactions, K. Tanaka, ed. (Wiley-VCH), pp. 229–276. https://doi.org/10.1002/9783527811908.ch10.

24. Wang, J., Blaszczyk, S.A., Li, X., and Tang, W. (2021). Transition metal-catalyzed selective carbon–carbon bond cleavage of vinylcyclopropanes in cycloaddition reactions. Chem. Rev. *121*, 110–139. https://doi.org/10.1021/acs.chemrev.0c00160.

25. Ganesh, V., and Chandrasekaran, S. (2016). Recent advances in the synthesis and reactivity of vinylcyclopropanes. Synthesis *48*, 4347–4380. https://doi.org/10.1055/s-0035-1562530.

26. Brownsey, D.K., Gorobets, E., and Derksen, D.J. (2018). Beyond geminal diesters: increasing the scope of metal-mediated vinylcyclopropane annulations while decreasing pre-activation. Org. Biomol. Chem. *16*, 3506–3523. https://doi.org/10.1039/C8OB00593A.

27. Jiao, L., and Yu, Z.X. (2013). Vinylcyclopropane derivatives in transition-metal-catalyzed cycloadditions for the synthesis of carbocyclic compounds. J. Org. Chem. *78*, 6842–6848. https://doi.org/10.1021/jo400609w.

28. Wender, P.A., Takahashi, H., and Witulski, B. (1995). Transition metal catalyzed [5 + 2] cycloadditions of vinylcyclopropanes and alkynes: a homolog of the Diels-Alder reaction for the synthesis of seven-membered rings. J. Am. Chem. Soc. *117*, 4720–4721. https://doi.org/10.1021/ja00121a036.

29. Jiao, L., Lin, M., and Yu, Z.X. (2010). Rh(I)-catalyzed intramolecular [3 + 2] cycloaddition reactions of 1-ene-, 1-yne- and 1-allene-vinylcyclopropanes. Chem. Commun. (Camb) *46*, 1059–1061. https://doi.org/10.1039/B922417C.

30. Jiao, L., Lin, M., and Yu, Z.X. (2011). Density functional theory study of the mechanisms and stereochemistry of the Rh(I)-catalyzed intramolecular [3+2] cycloadditions of 1-ene- and 1-yne-vinylcyclopropanes. J. Am. Chem. Soc. *133*, 447–461. https://doi.org/10.1021/ja107396t.

31. Lin, M., Kang, G.Y., Guo, Y.A., and Yu, Z.X. (2012). Asymmetric Rh(I)-catalyzed intramolecular [3 + 2] cycloaddition of 1-yne-vinylcyclopropanes for bicyclo[3.3.0] compounds with a chiral quaternary carbon stereocenter and density functional theory study of the origins of enantioselectivity. J. Am. Chem. Soc. *134*, 398–405. https://doi.org/10.1021/ja2082119.

32. Jiao, L., Lin, M., Zhuo, L.G., and Yu, Z.X. (2010). Rh(I)-catalyzed [(3 + 2) + 1] cycloaddition of 1-yne/ene-vinylcyclopropanes and CO: homologous Pauson-Khand reaction and total synthesis of (±)-α-agarofuran. Org. Lett. *12*, 2528–2531. https://doi.org/10.1021/ol100625e.

33. Lin, M., Li, F., Jiao, L., and Yu, Z.X. (2011). Rh(I)-catalyzed formal [5 + 1]/[2 + 2 + 1] cycloaddition of 1-yne-vinylcyclopropanes and two CO units: one-step construction of multifunctional angular tricyclic 5/5/6 compounds. J. Am. Chem. Soc. *133*, 1690–1693. https://doi.org/10.1021/ja110039h.

34. Liu, C.-H., Li, F., Yuan, Y., Dou, M., and Yu, Z.-X. (2018). Rh I-catalyzed intramolecular [3+2] cycloaddition of 1-allene-vinylcyclopropanes. Asian J. Org. Chem. *7*, 1609–1613. https://doi.org/10.1002/ajoc.201800294.

35. Quasdorf, K.W., and Overman, L.E. (2014). Catalytic enantioselective synthesis of quaternary carbon stereocentres. Nature *516*, 181–191. https://doi.org/10.1038/nature14007.

36. Long, R., Huang, J., Gong, J., and Yang, Z. (2015). Direct construction of vicinal all-carbon quaternary stereocenters in natural product synthesis. Nat. Prod. Rep. *32*, 1584–1601. https://doi.org/10.1039/C5NP00046G.

37. Hu, P., and Snyder, S.A. (2017). Enantiospecific total synthesis of the highly strained (−)-presilphiperfolan-8-ol via a pd-catalyzed tandem cyclization. J. Am. Chem. Soc. *139*, 5007–5010. https://doi.org/10.1021/jacs.7b01454.

38. Leggans, E.K., Barker, T.J., Duncan, K.K., and Boger, D.L. (2012). Iron(III)/NaBH4-mediated additions to unactivated alkenes: synthesis of novel 20′-vinblastine analogues. Org. Lett. *14*, 1428–1431. https://doi.org/10.1021/ol300173v.

39. Burés, J. (2016). A simple graphical method to determine the order in catalyst. Angew. Chem. Int. Ed. Engl. *55*, 2028–2031. https://doi.org/10.1002/anie.201508983.

40. Burés, J. (2016). Variable time normalization analysis: general graphical elucidation of reaction orders from concentration profiles. Angew. Chem. Int. Ed. Engl. *55*, 16084–16087. https://doi.org/10.1002/anie.201609757.

41. Le Gall, I.L., Laurent, P., Toupet, L., Salaün, J.-Y., and des Abbayes, H. (1997). Bridged hemilabile allylphosphonate ligand: synthesis and crystal structure of a new binuclear rhodium complex. Organometallics *16*, 3579–3581. https://doi.org/10.1021/om970182e.

42. Frisch, M.J., Trucks, G.W., Schlegel, H.B., Scuseria, G.E., Robb, M.A., Cheeseman, J.R., Scalmani, G., Barone, V., Mennucci, B., Petersson, G.A., et al. (2013). Gaussian 09, revision E.01 (Gaussian, Inc.).

43. Boese, A.D., and Martin, J.M.L. (2004). Development of density functionals for thermochemical kinetics. J. Chem. Phys. *121*, 3405–3416. https://doi.org/10.1063/1.1774975.

44. Weigend, F., and Ahlrichs, R. (2005). Balanced basis sets of split valence, triple zeta valence and quadruple zeta valence quality for H to Rn: design and assessment of accuracy. Phys. Chem. Chem. Phys. *7*, 3297–3305. https://doi.org/10.1039/B508541A.

45. Hehre, W.J., Radom, L., Schleyer, P.v.R., and Pople, J.A. (1986). *Ab Initio* Molecular Orbital Theory (Wiley).

46. Hay, P.J., and Wadt, W.R. (1985). *Ab initio* effective core potentials for molecular calculations. Potentials for the transition metal atoms Sc to Hg. J. Chem. Phys. *82*, 270–283. https://doi.org/10.1063/1.448799.

47. Marenich, A.V., Cramer, C.J., and Truhlar, D.G. (2009). Universal solvation model based on solute electron density and on a continuum model of the solvent defined by the bulk dielectric constant and atomic surface tensions. J. Phys. Chem. B *113*, 6378–6396. https://doi.org/10.1021/jp810292n.

48. Wang, Y., Liao, W., Wang, Y., Jiao, L., and Yu, Z.-X. (2022). Mechanism and stereochemistry of rhodium catalyzed [5 + 2 + 1] cycloaddition of ene−vinylcyclopropanes and carbon monoxide revealed by visual kinetic analysis and quantum chemical calculations. J. Am. Chem. Soc. *144*, 2624–2636. https://doi.org/10.1021/jacs.1c11030.

49. Jolly, R.S., Luedtke, G., Sheehan, D., and Livinghouse, T. (1990). Novel cyclization reactions on transition metal templates. The catalysis of intramolecular [4+2] cycloadditions by low-valent rhodium complexes. J. Am. Chem. Soc. *112*, 4965–4966. https://doi.org/10.1021/ja00168a055.

50. O'Mahony, D.J.R., Belanger, D.B., and Livinghouse, T. (2003). Substrate control of stereoselection in the rhodium(I) catalyzed intramolecular [4 + 2] cycloaddition reaction. Org. Biomol. Chem. *1*, 2038–2040. https://doi.org/10.1039/B302426C.

51. Gilbertson, S.R., and Hoge, G.S. (1998). Rhodium catalyzed intramolecular [4+2] cycloisomerization reactions. Tetrahedron Lett. *39*, 2075–2078. https://doi.org/10.1016/S0040-4039(98)00265-2.

52. Liao, W., and Yu, Z.-X. (2014). DFT study of the mechanism and stereochemistry of the Rh(I)-catalyzed diels–alder reactions between electronically neutral dienes and dienophiles. J. Org. Chem. *79*, 11949–11960v. https://doi.org/10.1021/jo5017844.

53. Neese, F. (2012). The ORCA program system. WIREs Comput. Mol. Sci. *2*, 73–78. https://doi.org/10.1002/wcms.81.

54. Neese, F. (2018). Software update: the ORCA program system, version 4.0. WIREs Comput. Mol. Sci. *8*, e1327. https://doi.org/10.1002/wcms.1327.

55. Riplinger, C., and Neese, F. (2013). An efficient and near linear scaling pair natural orbital based local coupled cluster method. J. Chem. Phys. *138*, 034106. https://doi.org/10.1063/1.4773581.

56. Riplinger, C., Sandhoefer, B., Hansen, A., and Neese, F. (2013). Natural triple excitations in local coupled cluster calculations with pair natural orbitals. J. Chem. Phys. *139*, 134101. https://doi.org/10.1063/1.4821834.